

Magnetic spectromicroscopy from Fe(100)

C. M. Schneider^{a)}

Physics Department, Simon Fraser University, Burnaby, B.C. V5A 1S6, Canada

K. Holldack,^{b)} M. Kinzler, and M. Grunze

Institut für Angew Physikalische Chemie, Universität Heidelberg, Im Neuenheimer Feld 253, D-69120 Heidelberg, Germany

H. P. Oepen

Institut für Grenzflächenforschung u. Vakuumphysik, KFA Jülich, D-52425 Jülich, Germany

F. Schäfers and H. Petersen

BESSY GmbH, Lentzeallee 100, D-14195 Berlin, Germany

K. Meinel and J. Kirschner

Max-Planck-Institut für Mikrostrukturphysik, Weinberg 2, D-06120 Halle/Saale, Germany

(Received 10 March 1993; accepted for publication 19 August 1993)

Magnetic domains on an Fe(100) surface have been imaged by means of energy-resolved photoemission microscopy. We excited the photoelectrons with circularly polarized synchrotron radiation in the soft x-ray region, and employed the effect of magnetic circular dichroism in the emitted photoelectrons in order to obtain contrast between differently oriented magnetic domains. This new approach offers a surface sensitive way to combine chemical and magnetic information on a microscopic scale.

Within the last decades photoelectron spectroscopy has been developed into a powerful tool in surface science. Nowadays, a great variety of physical problems may be addressed by this method, depending on the type of electronic states probed. Even the photoelectron spin has been made accessible to experimental investigations on both nonmagnetic and ferromagnetic materials.¹ Spin-split electronic states in ferromagnetic systems may be studied in great detail either by an explicit analysis of the photoelectron spin,² or by means of the recently reported magnetic circular dichroism in photoemission.³ Both approaches add magnetic sensitivity to conventional photoelectron spectroscopy. Still, with the advance of microtechnology comes yet another challenge. Present photoemission experiments usually sample a rather large surface area (of the order of several mm²), as determined by the size of the illuminated spot and the characteristics of the electron-optical system involved. The increasing importance and complexity of electronic and magnetic microstructures, however, requires improved lateral resolution capabilities. Considering the important role of photoelectron spectroscopy in the basic understanding of ferromagnetism, our objective was to develop a photoemission technique with magnetic sensitivity and high lateral resolution.

Our experimental approach to the problem employed a VG ESCASCOPE, which has been described in detail by Coxon *et al.*⁴ Briefly, the setup features a hemispherical energy analyzer in combination with an electrostatic input lens system. The instrument can be operated either in a spectroscopic mode as a conventional angle-resolving electron spectrometer, or in an imaging mode. The latter al-

lows the acquisition of photoelectron images with a spatial resolution $\Delta d < 10 \mu\text{m}$, using electrons of a well-defined kinetic energy. This energy filtering is an advantage over an immersion lens-type photoelectron microscope, which images on the basis of the total photoelectron yield.⁵ Our experiments were performed in an ultrahigh vacuum system (base pressure 1×10^{-10} mbar) at the German storage ring BESSY, using the elliptically polarized off-plane radiation dispersed by the SX-700-3 monochromator.⁶ The light was incident at 65° with respect to the surface normal of the sample, the degree of circular polarization being about $80\% \pm 5\%$ at photon energies $h\nu = 700\text{--}800$ eV.⁶ The photoemitted electrons were collected perpendicular to the photon beam within the plane of incidence. The samples consisted of several Fe(100) whiskers and an Fe(100) single crystal, the latter being mounted on a soft iron yoke which carried a wire coil. This arrangement allowed the sample to be brought into a well-defined state of magnetization for spectroscopy studies, and into a demagnetized state for imaging experiments.

In order to introduce magnetic sensitivity into the imaging process, we exploited the effect of x-ray magnetic circular dichroism in the emitted photoelectrons (MCDAD). In MCDAD, magnetic samples exhibit a difference in the intensity spectra recorded with circularly polarized light of opposite helicities. The specific form and structure of the energy distribution curve depends on the orientation of the sample magnetization \mathbf{M} with respect to the direction of the incident light (or equivalently, the photon spin σ) and the wave vector of the emitted photoelectrons \mathbf{k} .⁷ The dichroic signal is calculated from intensity spectra $I(E)$ taken at opposite \mathbf{M} or σ as the so-called intensity asymmetry A

$$A(E) = \frac{I_+(E) - I_-(E)}{I_+(E) + I_-(E)} \quad (1)$$

^{a)}On leave from Max-Planck-Institut für Mikrostrukturphysik, Weinberg 2, D-06120 Halle/Saale, Germany.

^{b)}Present address: BESSY GmbH, Lentzeallee 100, D-14195 Berlin, Germany.

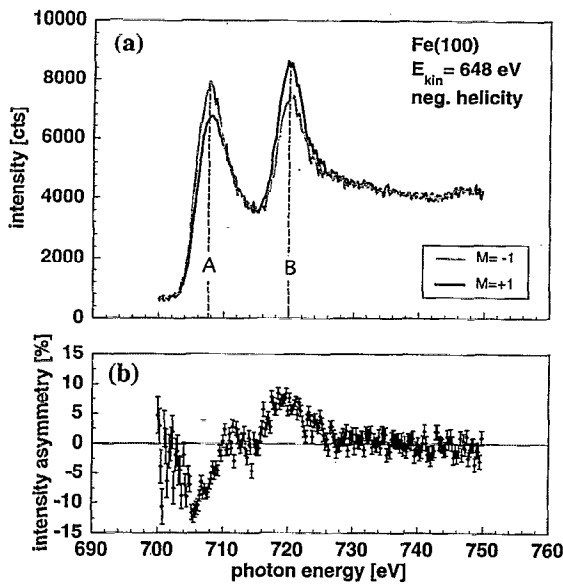


FIG. 1. Magnetic circular dichroism in the $L_3M_{23}V$ Auger electrons from iron as a function of photon energy. The constant final state spectra (a) have been taken with right hand circularly polarized light for sample magnetization antiparallel ($M = -1$) and parallel ($M = +1$) to the photon spin. The intensity asymmetry (b) is calculated according to Eq. (1).

Domains with different orientation relative to the incoming photon beam will thus give rise to a spatial variation of the energy-resolved photocurrent. This contrast may be optimized by tuning the energy filter to give the maximum value of A .

The explicit relation between photon spin direction σ , magnetization M , and dichroic asymmetry A depends distinctly on the kind of electrons analyzed in the experiment. It is complementary for directly photoemitted electrons and the so-called secondary electrons which have been emitted after a significant amount of inelastic scattering or by an Auger process. The specific magnetodichroic effects in the various emission channels can be employed to circumvent constraints in the experimental geometry. For instance, the dichroic signal in the direct photoemission channel exhibits a relatively complex angular variation which is caused by final state selection effects involving the electron wave vector k .^{8,9} This angular variation differs drastically from the simple relationship $A \sim (M \cdot \sigma)$ found in photoabsorption.¹⁰ Dichroic asymmetries of up to 10% in Fe $2p$ and $3p$ photoemission can be observed even for $M \perp \sigma$, if k is noncollinear with M or σ .⁸ The exploitation of this magnetodichroic effect in spectroscopy and imaging experiments requires both energy and angular resolution. Any experimental integration over k , e.g., by a partial yield measurement, will result in $A \sim (M \cdot \sigma)$.⁸

A further important finding is that magnetic circular dichroism appears also in the secondary electrons, e.g., from Auger excitations. This is demonstrated in Fig. 1(a), displaying the intensity of the $L_3M_{23}V$ Auger transition in Fe as a function of photon energy. The ESCASCOPE was operated in the spectroscopy mode and tuned to an electron energy of 648 eV with a bandwidth $\Delta E \approx 2$ eV. The two peaks at 708 (A) and 720 eV photon energy (B)

correspond to the photoexcitation thresholds of the $2p_{3/2}$ and $2p_{1/2}$ core levels. Magnetic circular dichroism causes the peak height of the spectral features to depend strongly on the direction of the Fe crystal's remanent magnetization M with respect to the photon spin σ . For the geometry chosen, $M = -1$ (shaded curve) corresponds to a magnetization direction with a large component antiparallel to σ , whereas $M = +1$ (solid curve) has a large component along σ . The intensity difference give rise to pronounced features in the asymmetry function [Fig. 1(b)]. The dichroic signal $A(E)$ has approximately the same size, but an opposite sign for the excitation with 708 and 720 eV photons. This gives rise to a peak-to-peak asymmetry of $\sim 20\%$. Switching the helicity of the light leads to a sign reversal in the asymmetry function. A qualitatively similar situation is observed at kinetic energies of 598 and 703 eV, corresponding to the $L_3M_{23}M_{23}$ and L_3VV Auger transitions in iron, respectively. Although we detect the Auger electrons with angular resolution, the information about the photoelectron wave vector k is lost during the Auger process. This makes the Auger electron emission a measure of the angle-integrated photocurrent. As a consequence, the relation of the dichroic asymmetry to the photon spin direction and sample magnetization is described by $A \sim (M \cdot \sigma)$.

The intensity asymmetry $A(E)$ forms the basis of a magnetic contrast in photoelectron images taken from magnetic surfaces. It will cause magnetic domains which are oriented parallel and antiparallel to the photon spin to appear with different intensities, i.e., with different grey levels in a grey scale representation. Figure 2 displays images from an "L"-shaped Fe(100) whisker, which have been recorded using L_3VV Auger electrons excited with light of negative helicity. The photon energies were chosen as $h\nu = 708$ eV [Fig. 2(a)] and $h\nu = 720$ eV [Fig. 2(b)], corresponding to the $2p_{3/2}$ and $2p_{1/2}$ excitation resonances. The direction of light incidence is along the vertical (y -) axis of the images. Each image required about 5 min acquisition time. Common to both images is a dark spot close to the elbow of the L. As a local X-ray photoemission spectroscopy analysis of this spot showed the contrast was not of chemical origin, it is tentatively attributed to a defect in the otherwise very flat surface topography. The magnetic contribution to the contrast already appears in these raw data as a pattern of differently shaded areas. The vertical leg of the whisker in Fig. 2(a) (figure in the following denoted as A), for instance, shows a dark and a light shaded part, which are separated by a straight vertical boundary. This contrast, which is due to two 180° domains, is inverted in Fig. 2(b) (B), but disappears in the sum of the two images $\{B+A\}$ [Fig. 2(c)]. We may extract the magnetic information by forming the asymmetry function of the two images $\{B-A\}/\{B+A\}$, in close analogy to Eq. (1). The result is shown in Fig. 2(d), and displays the magnetic domain pattern on the surface of the iron whisker. Regions with a magnetization vector M_y antiparallel (parallel) to the incoming light appear dark (white), whereas a magnetization vector M_x perpendicular to the incoming light gives rise to an intermediate grey level. A distinction between M_x and $-M_x$ requires the sample to be

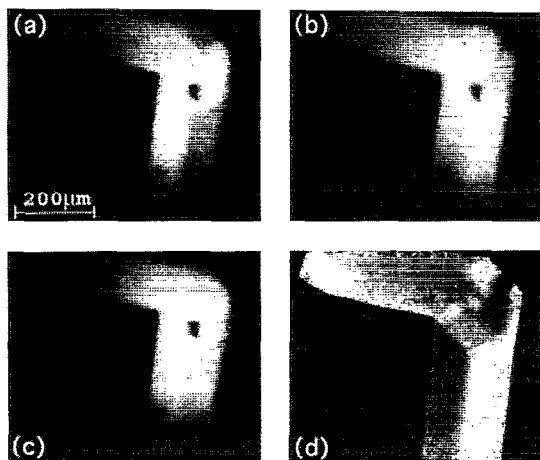


FIG. 2. Spectromicroscopy from an iron whisker using L_3VV Auger electrons. The images have been recorded with right-hand circularly polarized light of 708 (a) and 720 eV photon energy (b), the light being incident along the vertical axis of the images. The sum (c) and the normalized difference (d) of the raw images, as obtained by image processing, show the topographic (c) and magnetic contribution (d) to the total contrast. Dark (white) areas in (d) represent domains with a magnetization vector pointing upwards (downwards) along the vertical axis. Domains which are shown in a medium grey level have their magnetization vector along the horizontal axis.

rotated with respect to the incoming light so that some projection of the magnetization along the y direction exists, which can give rise to a sizable contrast. The same domain pattern has been observed using $L_3M_{23}M_{23}$ and $L_3M_{23}V$ Auger and $3p$ photoelectrons. Finally we note that Fig. 2(d) shows a more complicated arrangement of domains than is seen from straight iron whiskers.¹¹ This may be partly caused by the above-mentioned defect in the elbow region. The defect itself is centered in a domain with a magnetization along the x axis. Furthermore, the particular shape of the elbow itself may give rise to local demagnetizing fields, and thus to a complex pattern of closure domains.

With its presently available spatial resolution of about $10 \mu\text{m}$, the above experimental approach has no ambitions to compete with other well-established domain imaging techniques, such as scanning electron microscopy with spin polarization analysis or optical Kerr microscopy. Its main advantage lies in the unique combination of spectroscopic (i.e., elemental and chemical specificity) and magnetic information, which may be obtained on a microscopic scale. Since both the photon energy and the kinetic energy of the electrons may be chosen independently, the chemical and magnetic signal can be obtained almost without background. This is an important difference to scanning electron beam methods which achieve a far better lateral resolution, but require a spin analysis of the electron-beam-induced Auger electrons. These Auger electrons are usually accompanied by a highly spin polarized background of inelastically scattered electrons, and their spin polarization must be carefully extracted by suitable procedures in order to separate the magnetic information.¹² The low signal-to-noise ratio introduces significant complica-

tions in the imaging process. A further interesting aspect is the parallel data acquisition in the ESCASCOPE through which, in combination with high brilliance light sources such as undulators or similar magnetic insertion devices, real-time imaging becomes feasible.

Compared to recent studies of magnetic domains with an immersion lens photoelectron microscope,¹³ our angle- and energy-resolved approach has several advantages. First, it can fully exploit the different forms of magnetic dichroism in direct photoemission and secondary electron emission. By tuning the electron energy from photoelectrons over the associated Auger excitations down to the low-energy secondary electrons, one obtains a very detailed picture of their individual contributions to the magnetism. Second, the specific angular dependencies of the various magnetodichroic effects can be used to compensate for possible geometrical restrictions of the experimental setup. By combining measurements employing magnetic dichroism phenomena with circularly and linearly polarized light,¹⁴ the complete domain pattern at a surface may be obtained on the basis of only three raw images without the need to rotate the sample. Third, one may deliberately introduce an additional depth selectivity into the measurements by analyzing electrons of very different kinetic energies. These virtues suggest that magnetic spectromicroscopy on the basis of magnetodichroic phenomena will become an interesting new tool in surface and thin film magnetism.

We are indebted to Dr. B. Heinrich and Dr. Z. Celinski for providing us with the iron whiskers. This work was supported by the Bundesminister für Forschung und Technologie through Grants No. 05-5-EFAA-I-5 and No. FKZ-055VHFX1. C.M.S. acknowledges financial support of the Deutscher Akademischer Austauschdienst under Grant No. 516-401-514-3 during his stay at Simon Fraser University.

¹U. Heinzmann and G. Schönhense, in *Polarized Electrons in Surface Physics*, edited by R. Feder (World Scientific, Singapore, 1985).

²E. Kisker, in *Metallic Magnetism*, edited by H. Capellmann (Springer, Berlin, 1987).

³C. M. Schneider, D. Venus, and J. Kirschner, *Proceedings of the 10th International Conference on Vacuum Ultraviolet Radiation*, Paris 1992 (World Scientific, Singapore, 1993) (to be published).

⁴P. Coxon, J. Krizek, M. Humpherson, and I. R. M. Wardell, *J. Electron Spectrosc. Rel. Phenom.* **51/52**, 821 (1990).

⁵B. P. Tonner and G. R. Harp, *Rev. Sci. Instrum.* **59**, 835 (1988).

⁶J. Bansmann, Ch. Ostertag, G. Schönhense, F. Fegel, C. Westphal, M. Getzlaff, F. Schäfers, and H. Petersen, *Phys. Rev. B* **46**, 13496 (1992).

⁷L. Baumgarten, C. M. Schneider, H. Petersen, F. Schäfers, and J. Kirschner, *Phys. Rev. Lett.* **65**, 492 (1990); C. M. Schneider, D. Venus, and J. Kirschner, *Phys. Rev. B* **45**, 5041 (1992).

⁸D. Venus, C. M. Schneider, J. Kirschner, L. Baumgarten, and C. Boeglin, *J. Phys.: Condens. Matter* **5**, 1239 (1993).

⁹G. van der Laan, M. A. Hoyland, M. Surman, C. F. J. Flipse, and B. T. Thole, *Phys. Rev. Lett.* **69**, 3872 (1992).

¹⁰G. Schütz, W. Wagner, W. Wilhelm, P. Kienle, R. Zeller, R. Frahm, and G. Materlik, *Phys. Rev. Lett.* **58**, 737 (1987).

¹¹D. J. Craik and R. S. Tebble, *Ferromagnetism and Ferromagnetic Domains* (Wiley, New York, 1965).

¹²M. Landolt, in *Polarized Electrons in Surface Physics*, edited by R. Feder (World Scientific, Singapore, 1985).

¹³J. Stöhr, Y. Wu, M. G. Sarmant, B. D. Hermsmeier, G. Harp, S. Koranda, D. Dunham, and B. P. Tonner, *Science* **259**, 658 (1993).

¹⁴Ch. Roth, F. U. Hillebrecht, H. B. Rose, and E. Kisker, *Phys. Rev. Lett.* **70**, 3479 (1993).